Journal of Pharmaceutical Sciences xxx (2016) 1-11

Contents lists available at ScienceDirect

Journal of Pharmaceutical Sciences

journal homepage: www.jpharmsci.org

Pharmaceutics, Drug Delivery and Pharmaceutical Technology

Host-Guest Complexes of Carboxylated Pillar[*n*]arenes With Drugs

Nial J. Wheate [1, *], Kristie-Ann Dickson [2], Ryung Rae Kim [1], Alireza Nematollahi [1], René B. Macquart [3], Veysel Kayser [1], Guocan Yu [4], W. Bret Church [1], Deborah J. Marsh [2]

[1] *Faculty of Pharmacy, University of Sydney, Sydney, NSW 2006, Australia*
[2] *Hormones and Cancer Group, Kolling Institute of Medical Research, Royal North Shore Hospital, University of Sydney, St Leonards, NSW 2065, Australia*
[3] *School of Chemistry, University of Sydney, Sydney, NSW 2006, Australia*
[4] *State Key Laboratory of Chemical Engineering, Department of Chemistry, Zhejiang University, Hangzhou 310027, People's Republic of China*

ARTICLE INFO

Article history:
Received 29 May 2016
Revised 7 September 2016
Accepted 12 September 2016

Keywords:
pillar[*n*]arene
drug delivery
fluorescence
biodiagnostics
host-guest
nanocapsule
molecular modeling
excipient
pharmaceutics

ABSTRACT

Pillar[*n*]arenes are a new family of nanocapsules that have shown application in a number of areas, but because of their poor water solubility their biomedical applications are limited. Recently, a method of synthesizing water-soluble pillar[*n*]arenes was developed. In this study, carboxylated pillar[*n*]arenes (WP[*n*], $n = 6$ or 7) have been examined for their ability to form host-guest complexes with compounds relevant to drug delivery and biodiagnostic applications. Both pillar[*n*]arenes form host-guest complexes with memantine, chlorhexidine hydrochloride, and proflavine by ^{1}H nuclear magnetic resonance and modeling. Binding is stabilized by hydrophobic effects within the cavities, and hydrogen bonding and electrostatic interactions at the portals. Encapsulation within WP[6] results in the complete and efficient quenching of proflavine fluorescence, giving rise to "on" and "off" states that have potential in biodiagnostics. The toxicity of the pillar[*n*]arenes was examined using *in vitro* growth assays with the OVCAR-3 and HEK293 cell lines. The pillar[*n*]arenes are relatively nontoxic to cells except at high doses and after prolonged continuous exposure. Overall, the results show that there could be a potentially large range of medical applications for carboxylated pillar[*n*]arene nanocapsules.

Introduction

Nanocapsules are short polymers which close to form ring or barrel-shaped 3-dimensional (3D) structures which are useful in host-guest chemistry and have a range of important applications.[1] They are particularly useful in medicine and biodiagnostics where they have been shown to improve drug chemical and physical stability, as well as the solubility, dissolution, and effectiveness of drugs. They have also been shown to act as antidotes, work as *in vivo* chemical extractors, induce pKa shifts of drug acid and base functional groups, mask drug taste, reduce drug toxicity, and even reverse drug resistance.[1-3]

To date, 3 nanocapsule families have been extensively examined for their biomedical applications: *n*-cyclodextrins,[4] cucurbit[*n*]urils,[5] and calix[*n*]arenes,[6] where *n* indicates the number of subunits of each different-sized nanocapsule. *n*-Cyclodextrins are approved for use in medicines,[7] and are included in a number of pharmaceutical formulations, including the antifungal drug itraconazole, the antipsychotic drug aripiprazole, and maropitant which is used to control motion sickness and nausea in animals.

Pillar[*n*]arenes are a new nanocapsule family that was first reported in 2008 (Fig. 1a).[8] They are synthesized from the Lewis-catalyzed reaction of paraformaldehyde and 1,4-dimethoxybenzene and form a range of different-sized nanocapsules with a roughly symmetrical, pillar-like shape.[9] The cavities of the pillar[*n*]arenes are able to store and release small molecules and can be easily modified and functionalized. While they have been utilized as components in a variety of supramolecular- and nano-based drug delivery machines,[10-13] they have not been extensively studied in their own right as simple drug delivery vehicles, nor have they been examined for their use in biodiagnostics.

Native pillar[*n*]arenes are soluble only in organic solvents (methanol, acetone, acetonitrile, dimethylformamide, and dimethylsulfoxide) and display no significant water solubility.[8] This has recently been overcome through conversion of the hydroxyl groups to carboxylates on the pillar[*n*]arenes' rings (Fig. 1b).[14]

Conflicts of interest: The authors declare no conflicts of interest.
This article contains supplementary material available from the authors by request or via the Internet at http://dx.doi.org/10.1016/j.xphs.2016.09.008.

* *Correspondence to:* Nial J. Wheate (Telephone: +61 2 9036 7647; Fax: +61-2-9351-4391).
E-mail address: nial.wheate@sydney.edu.au (N.J. Wheate).

http://dx.doi.org/10.1016/j.xphs.2016.09.008
0022-3549/

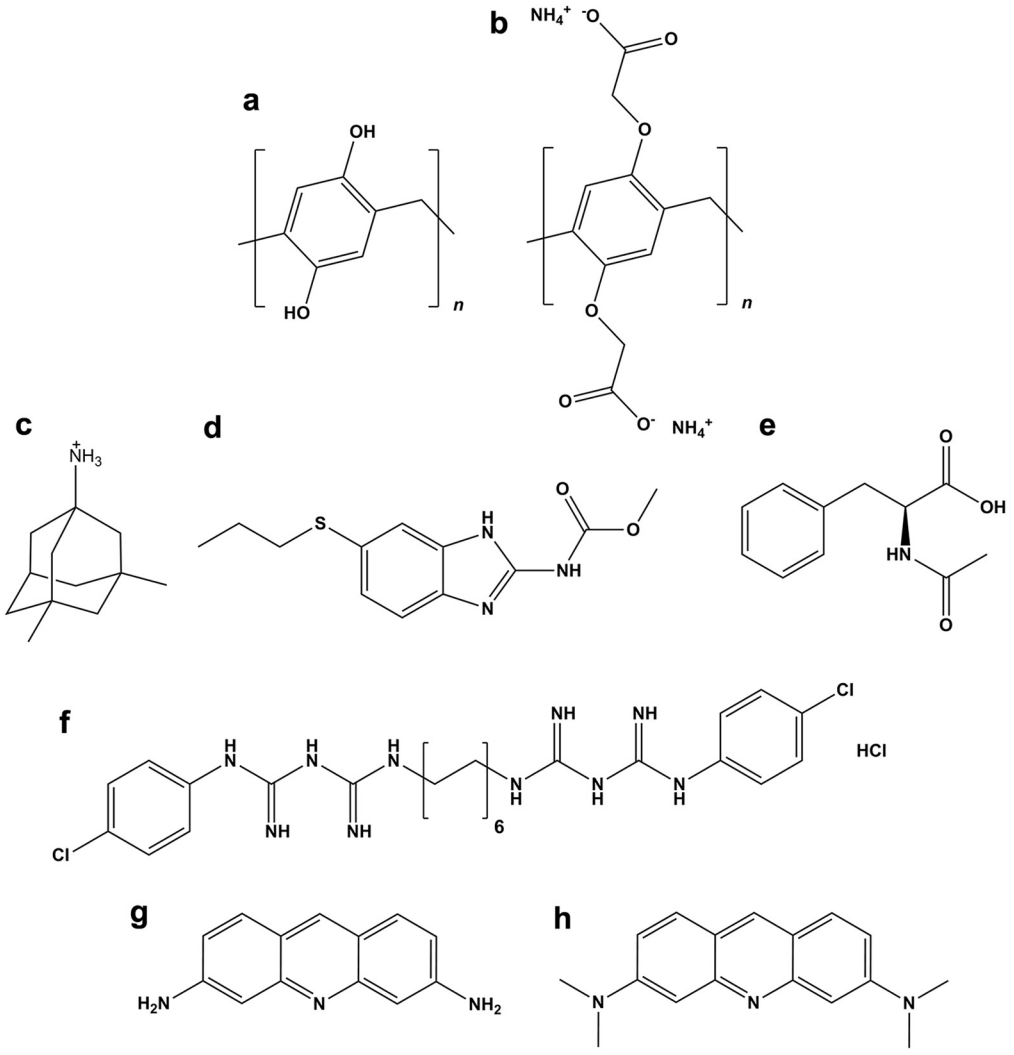

Figure 1. The chemical structures of (a) native and (b) carboxylated pillar[*n*]arenes (WP[*n*], $n = 5$, 6, or 7), and the biorelevant compounds used in this study: (c) memantine, (d) albendazole, (e) *N*-acetyl-phenylalanine, (f) chlorhexidine hydrochloride, (g) proflavine, and (h) acridine orange.

These carboxylated pillar[*n*]arenes (WP[*n*]) are anionic and can have a charge up to 10^- or 14^- depending on the number of subunits and the pH of the solution. As such, they display excellent water solubility, and because of this, may have conceivable medical applications.

Carboxylated pillar[*n*]arenes have several potential benefits over other nanocapsule families. First, they are more easily functionalized and are more water soluble compared with cucurbit[*n*]urils. Second, they can form stronger host-guest complexes, and it is easier to monitor their host-guest complex interactions, compared with *n*-cyclodextrins. Third, the barrel shape of carboxylated pillar[*n*]arenes provides a more suitable cavity for the storage, protection, and release of guests, compared with the bowl shape of the calix[*n*]arenes.

In this study, we have examined the potential of water-soluble carboxylated pillar[*n*]arenes with respect to their application in drug delivery and biodiagnostics. The formation of host-guest complexes with a range of biorelevant molecules was examined by ^{1}H nuclear magnetic resonance (NMR), molecular modeling, and fluorescence spectrophotometry, and their toxicity determined using *in vitro* growth inhibition assays.

Materials and Methods

Materials

The carboxylated pillar[*n*]arenes ($n = 6$ or 7) were made as previously described.[14] Memantine, proflavine, acridine orange, and *N*-acetyl-phenylalanine were purchased from Sigma-Aldrich (Sydney, Australia). Chlorhexidine hydrochloride was purchased from Imperial Chemical Laboratories Ltd (London, UK). Albendazole was provided by Dr. Anthony Day (UNSW, Australia). Deuterium chloride (99.9%) was purchased from Cambridge Isotope Laboratories, Inc. (Tewksbury, MA).

NMR

^{1}H NMR spectra were recorded on a Varian Avance 400 in D_2O. One-dimensional spectra were obtained using 128-512 scans. Two-dimensional rotating frame Overhauser effect spectroscopy (ROESY) experiments were undertaken using 200 $t1$ increments with 64 scans per increment, a mix time of 200 ms and a relaxation delay of 1 s.

Fluorescence

Fluorescence experiments were conducted using a Shimadzu RF-5301 RC spectrofluorometer. Solutions (3 mL) of proflavine or acridine orange and WP[6] were prepared to give a final dye concentration of 30 μM and a WP[6] concentration between 0 and 60 μM in increments of 5 μM for WP[6]. An excitation wavelength of 451 nm was used and emission was measured between 490 and 550 nm; emission maxima was 508 nm. The results were graphed as fluorescence intensity (arbitrary units) as a function of WP[6] concentration.

Fluorescence lifetime measurements were conducted with an Edinburgh Instrument Lifespec-blue F900 using the time-correlated single photon counting method as described previously.[15] Briefly, the excitation source was a vertically polarized picosecond diode laser, lasing at 475 nm. Fluorescence decays were collected at 54.7° to avoid rotational contributions using 4096 channels and analyzed via Marquardt-Levenberg algorithm,[16] using a single exponential curve fit with $I = \alpha \cdot exp(-\tau/t)$, where α is the pre-exponential factor and τ is the fluorescence lifetime. Goodness of the curve fit was judged by the reduced residuals and χ^2 statistics.

Molecular Modeling

Molecular modeling of the carboxylated pillar[*n*]arenes ($n = 5$, 6, and 7), with and without guests—memantine, chlorhexidine hydrochloride, and proflavine—were conducted using AutoDock Vina.[17] Carboxylated pillar[*n*]arene structures were constructed using a published crystal structure of WP[5][18] as a scaffold, and were further optimized and validated through an energy minimization macro on YASARA version 15.8.24.[19] The AutoDockTools[20] and the Python-based Molecular Viewer were used to prepare both the 3D structure of the carboxylated pillar[*n*]arenes as rigid macromolecules and the guest molecules, with all torsions allowed wherever available. Polar hydrogens were added before the Gasteiger charges and atomic solvation parameters were assigned, followed by computation of the grid maps. A grid spacing of 1.0 Å, within a 3D space measuring 30 × 15 × 15 Å, which was sufficiently large to accommodate both the carboxylated pillar[*n*]arenes and the guests, was deployed at the center of each nanocapsule. The exhaustiveness parameter for the AutoDock Vina value was set at 16. In order to examine the validity of the docking, hydrogen bonds and van der Waals interactions between the carboxylated pillar[*n*]arenes and the guests were analyzed with AutoDockTools.[20,21] Rendering of the images was performed using the PyMOL Molecular Graphics System. Manuscript figure production and analysis of the final bonding interactions between the nanocapsules and guests was undertaken using Accelrys Software, Inc., Discovery Studio version 3.1.1.11157.

Cell Lines

Human embryonic kidney (HEK293) and OVCAR-3 high-grade serous ovarian cancer cells were purchased from the American Type Culture Collection (Manassas, VA). The HEK293 cells were maintained in Dulbecco's modified eagle medium (HyClone #SH30243; GE Healthcare Life Sciences, Parramatta, Australia) and the OVCAR-3 cells in RPMI 1640 (HyClone #SH30027; GE Healthcare Life Sciences), both supplemented with 10% fetal calf serum (AusGeneX, Molendinar, Australia) and incubated at 37°C in a humidified 5% CO_2 atmosphere. Cell line identity was authenticated by short tandem repeat profiling using the AmpFLSTR® Identifiler® PCR Amplification Kit (Applied Biosystems), and a 16 loci (15 short tandem repeat loci plus Amelogenin) STR multiplex kit provided by CellBank Australia (Westmead, Australia).

Cell Proliferation Assays

Assessment of cell proliferation in real time was carried out using an IncuCyte™ FLR Imaging System (Essen BioScience, Ann Arbor, MI). The cells (4×10^3/well for HEK293 cells or 5×10^3/well for OVCAR-3 cells) were dispensed into 96-well plates in 100 μL of culture medium. Stock solutions of WP[6], WP[7], and β-cyclodextrin (10 mM) were diluted into culture medium and 100 μL was added at specified doses (10, 25, 50, 100, 250, or 500 μM final concentration) after the cells had attached (~4-5 h). Plates were transferred to the IncuCyte™ apparatus and incubated for 78 h. Images (1 per well) were collected every 3 h.

Statistical Analysis

Data analysis was performed using SPSS version 22.0 (SPSS Australasia Pty Ltd., Chatswood, Australia). Data are expressed as mean ± SEM. Statistical significance for the cell proliferation assays was determined by repeated measurements using analysis of variance with a Fisher least significance difference *post hoc* test; $p < 0.05$ was considered statistically significant.

Results and Discussion

Every dosage form (e.g., tablets, injections, creams) contains 2 types of components: the active pharmaceutical ingredient (the drug molecule) and the excipients which are added to the dosage forms to ensure they perform as desired. We are interested in the biomedical applications of carboxylated pillar[*n*]arenes as pharmaceutical excipients rather than as active pharmaceutical ingredients. In this way, we envisage that carboxylated pillar[*n*]arenes may be added to different dosage forms for a variety of applications, such as drug stabilization, drug delivery, or to improve bioimaging.

Therefore, our goal was to determine what types of molecules form host-guest complexes with carboxylated pillar[*n*]arenes, what structural features drive this binding, provide proof-of-concept for a potential biomedical application, and undertake some preliminary safety testing.

The first step in the research was to identify whether any biorelevant molecules formed host-guest complexes with carboxylated pillar[*n*]arenes, and determine the factors and forces involved in their formation. Three compounds were selected that varied in both their structure and their pharmaceutical application. Memantine is a small organic drug that is used in the treatment of Alzheimer's disease, whereas chlorhexidine is a preservative found in a variety of different dosage forms.[7] Proflavine is a typical acridine-based dye that is used in diagnostics. Dyes are also commonly used to track drug movement into cells and whole organs, and to mark specific biological molecules, like proteins and DNA.

Formation of Host-Guest by ^1H NMR

The formation of host-guest complexes of memantine, chlorhexidine hydrochloride, and proflavine with WP[6] and WP[7] have been examined by ^1H NMR. The spectra of free WP[6] and WP[7] in D_2O show 3 nonexchangeable resonances (Fig. 2). The protons of the aromatic ring (12-14 hydrogens depending on the number of subunits) are magnetically equivalent and appear as a single resonance around 6.5 ppm. The methylene protons of the carboxylate arms are observed around 4.1 ppm, whereas the protons of the

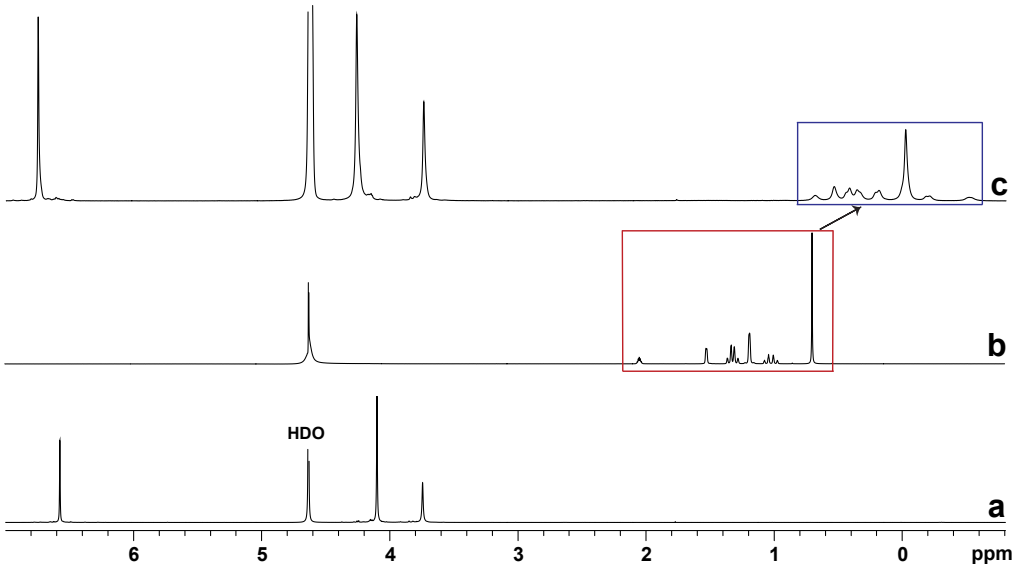

Figure 2. The ^{1}H NMR (D_2O, 400 MHz) spectra of (a) free WP[6], (b) free memantine, and (c) an equimolar concentration of WP[6] and memantine showing the large upfield shifts of the drug resonances on encapsulation inside the highly shielding environment of the WP[6] cavity.

bridging methylene groups between the phenolic rings are observed around 3.8 ppm.

Memantine

An organic salt of memantine has previously been studied with per-ethylated-pillar[*n*]arenes in nonaqueous solvents and been found to bind within the cavities of the nanocapsules.[22] In this study, we found that memantine also binds into the cavities of WP[6] and WP[7]. Free memantine has 6 resonances between 0.7 and 2.05 ppm and upon the addition of one mole equivalent of WP[6] all the drug resonances shift upfield to between −0.52 and 0.69 ppm (Figs. 2 and Supplementary Fig. S1). The magnitude of the shifts is larger than those observed on memantine binding within the cavity of cucurbit[7]uril which results in drug resonances in the region 0.1-1.7 ppm.[23] The methyl resonance of memantine is easily distinguished in the spectra and moves upfield by 0.72 ppm upon binding by WP[6]. The encapsulation of memantine within WP[6] also results in small chemical shift changes of the nanocapsule's peaks. Both the aromatic proton resonance and the carboxylate methylene proton resonance move downfield by 0.18 ppm, but the resonance for the bridging methylene protons remains unmoved at 3.74 ppm.

Similar to WP[6], the addition of WP[7] to memantine results in upfield shifts of the drug's proton resonances (Supplementary Fig. S1). The addition of 0.5 mole equivalent of WP[7] shifts the memantine peaks from 0.7-2.05 ppm to 0.16-1.44 ppm. Addition of more WP[7] to a 1:1 ratio with memantine further shifts the drug peaks to the region −0.02 to 0.94 ppm. For the 1:1 complex, the memantine methyl resonance, which is easiest to track, moves 0.54 ppm which is a smaller shift compared with WP[6]. The continual upfield shift of the drug's proton resonances with increasing WP[7] concentration indicates that the binding kinetics are fast on the NMR timescale.

The host-guest complexes of pillar[*n*]arenes are also able to be examined in more detail using 2-dimensional ^{1}H NMR, which is difficult to undertake for some nanocapsules, like cucurbit[*n*]urils. Drug, excipient, or dye protons located within the cavity of carboxylated pillar[*n*]arenes can give thorough space cross peaks to the nanocapsule's aromatic and bridging methylene protons. As an example, a ROESY spectrum of WP[6] and memantine shows several intramolecular cross peaks between protons of the nanocapsule, but also intermolecular cross peaks from the memantine's methyl protons to both the WP[6] aromatic and methylene peaks (Supplementary Fig. S2).

Chlorhexidine Hydrochloride

The ^{1}H NMR of chlorhexidine displays 5 resonances: 2 in the aromatic region representing the 2 protons of the chlorophenyl groups (7.09 and 7.24 ppm), and 3 aliphatic resonances for the protons of the hexamethylene chain of the excipient (2.95, 1.30, and 1.11 ppm).

The addition of one mole equivalent of WP[7] to a solution of chlorhexidine results in upfield shifts of the excipient's aromatic and aliphatic resonances (Fig. 3). The chlorophenyl peaks move to 6.31 and 6.43 ppm, shifts of 0.78 and 0.81 ppm, respectively, which indicates that they are located deep within the cavity of the nanocapsule. Likewise, the excipient's aliphatic resonances also shift upfield giving 4 new resonances at 1.65, 1.38, −0.23 and −0.66 ppm. The magnitude of these shifts (~1.3-1.6, 1.53, and 1.77 ppm, respectively) indicate that the protons are also deep within the WP[7] cavity. The addition of another mole equivalent of WP[7] to the chlorhexidine to give a host-guest ratio of 2:1 results in no further significant shifts of the chlorhexidine resonances (<0.05 ppm), which indicates that it forms only a 1:1 host-guest complex.

The results for chlorhexidine and WP[7], where both the excipient's aromatic and aliphatic proton resonances shift upfield, indicate that 2 types of binding to chlorhexidine may be possible. The first type of binding involves the WP[7] shuttling quickly between 2 binding sites: over the hexamethylene chain, then out to the chlorophenyl groups and then back to the central chain. Alternatively, the cavity of WP[7] is of a sufficient size to allow bending of the chlorhexidine so that it can fold back onto itself. This folding would allow both the chlorophenyl groups and the hexamethylene chain to be located within the cavity of the nanocapsule at the same time.

Proflavine

The dye proflavine has 4 aromatic peaks in its ^{1}H NMR at 6.35, 6.78, 7.52, and 8.33 ppm (Fig. 4). The addition of one mole

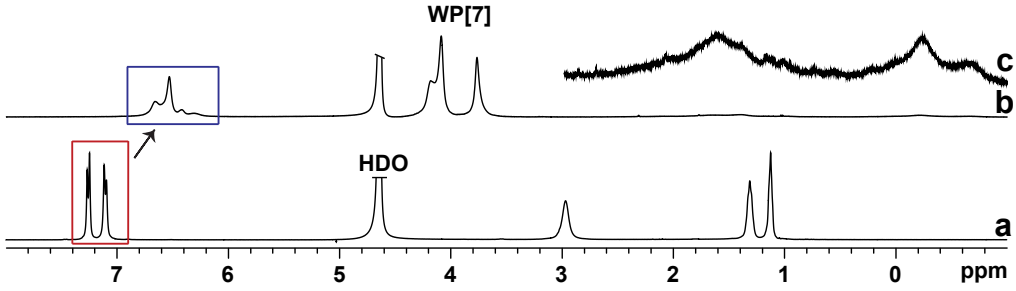

Figure 3. The ^{1}H NMR (D_2O, 400 MHz) spectra of (a) free chlorhexidine hydrochloride, (b) chlorhexidine hydrochloride with one mole equivalent of W[7] showing the upfield shift of the chlorophenyl resonances from 7.1-7.3 to 6.3-6.7 ppm, and (c) expansion of the aliphatic region of chlorhexidine and WP[7] showing the broadness of the chlorhexidine aliphatic peaks on encapsulation within the nanocapsule.

equivalent of WP[6] results in significant changes in the spectra of both the nanocapsule and the dye resonances. All the peaks are significantly broadened and move upfield and only 2 proflavine peaks are now observed—at 6.33 and 5.13 ppm—representing a shift of at least 1.22 ppm for the H_a resonance.

Similar but distinctively different changes are observed in the ^{1}H NMR of proflavine with one mole equivalent of WP[7] (Fig. 4). Again, all resonances are significantly broadened and move upfield, but there are 3 observable proflavine peaks, an apparent doublet at 6.24 ppm with the other 2 resonances at 5.96 and 5.41 ppm.

As encapsulation within the cavity of the carboxylated pillar[*n*]arenes has a shielding effect on guest protons, their resonances shift upfield in ^{1}H NMR spectra. If there were sections of proflavine not inside the WP[6] or WP[7] cavities, then their proton resonances would not shift upfield, and in fact would be deshielded and move slightly downfield. As this is not observed, we conclude that the proflavine is completely encapsulated within the nanocapsules.

Molecular Modeling

Models of memantine, chlorhexidine, and proflavine with WP[6] and WP[7] were generated to better understand the host-guest chemistry of these molecules. For comparison, each guest was also modeled with WP[5].

Memantine

This drug is too large to fit within the cavity of WP[5] and instead interacts weakly with the aromatic rings on the nanocapsule's surface (Supplementary Fig. S4). The models of memantine with WP[6] and WP[7] show that the drug can be completely encapsulated within the cavity of the larger carboxylated pillar[*n*]arenes (Fig. 5). Each host-guest complex is stabilized by a single hydrogen bond from a memantine amine hydrogen to an ether oxygen in WP[6] (H-bond length 2.11 Å) or to a carboxylate hydrogen in WP[7] (2.34 Å).

The WP[6] model is also consistent with the ROESY NMR spectrum of the nanocapsule with memantine. At the orientation

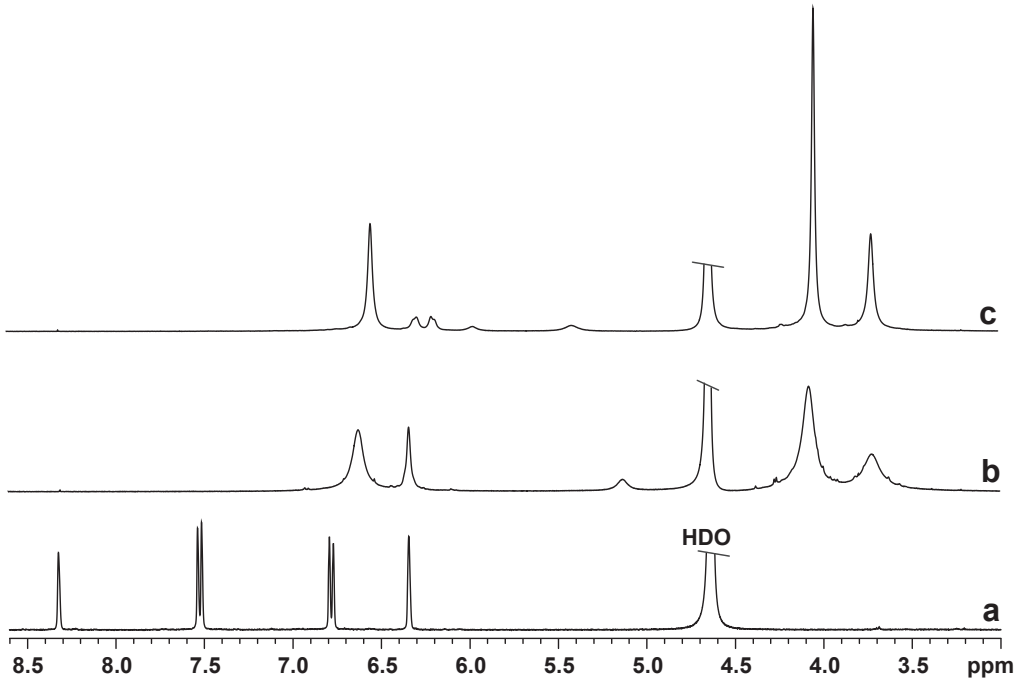

Figure 4. The ^{1}H NMR (D_2O, 400 MHz) spectra of (a) free proflavine, (b) proflavine with one mole equivalent of WP[6], and (c) proflavine with one mole equivalent of WP[7]. The spectra show the large upfield shifts and broadening of the proflavine resonances on encapsulation by the nanocapsules.

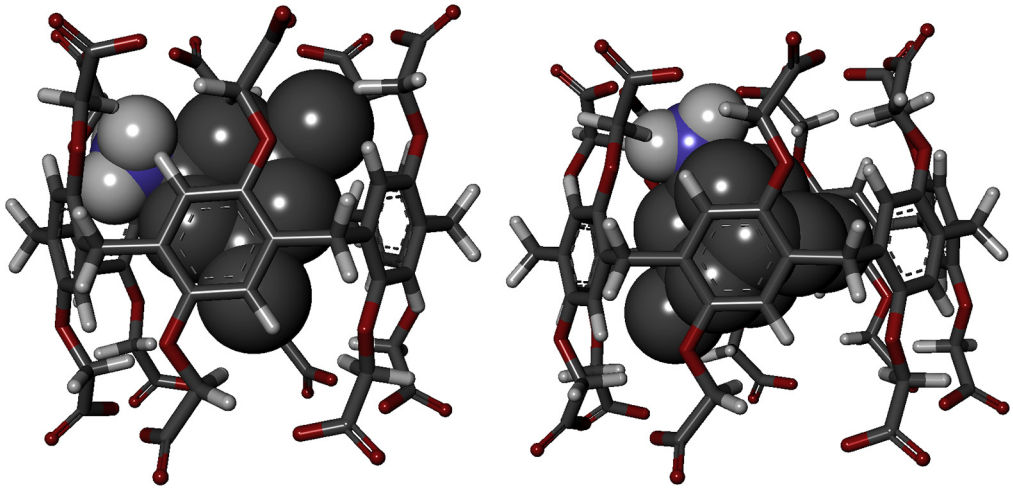

Figure 5. Molecular models of memantine with (left) WP[6] and (right) WP[7] showing the complete encapsulation of the drug within the nanocapsules. Binding is stabilized through hydrophobic effects within the cavity and a hydrogen bond from a memantine amine proton to the ether or carboxylate oxygen in the arms of the carboxylated pillar[*n*]arenes.

shown, both methyl resonances of the drug are close to an aromatic proton of the WP[6] at distances of 2.05 and 2.57 Å, respectively, and to the methylene protons of the carboxylate arms of the nanocapsule with distances of 1.49-2.29 Å which places the protons at a sufficiently short distance that they would be expected to give cross peaks in ^{1}H-^{1}H ROESY spectra, which is consistent with the cross peaks seen in Supplementary Figure S2.

Chlorhexidine Hydrochloride

Molecular modeling of chlorhexidine with the carboxylated pillar[*n*]arenes shows differences in the binding modes between the different-sized nanocapsules. A model of WP[5] with the excipient shows that the chlorhexidine is bound by the nanocapsule over the central hexamethylene chain (Supplementary Fig. S5). The narrow width of the WP[5] cavity means the chain is fully elongated through the cavity, with no folding or bending.

A similar mode of binding is seen between chlorhexidine and WP[6] where binding again occurs over the excipient's central chain; however, the larger cavity allows for a certain degree of freedom in the orientation of the chain which is seen to partially bend back upon itself (Fig. 6). Interestingly, the chlorhexidine-WP[6] host-guest complex is stabilized by 6 separate hydrogen bonds, 3 at each portal. These bonds range in length from 2.11 to 2.48 Å.

In contrast, the binding of chlorhexidine and WP[7] shows an unusual ability of the excipient to bend back completely upon itself so that both the central hexamethylene chain and the 2 terminal chlorophenyl groups are located within the nanocapsule's cavity simultaneously. This model of the host-guest complex is consistent with the ^{1}H NMR spectrum which showed upfield shifts of both the methylene and aromatic chlorhexidine resonances upon the addition of WP[7]. The WP[7]-based host-guest complex is stabilized by 4 hydrogen bonds (1.96-2.38 Å), 2 at each portal, and a less common chloride—NH bond (2.42 Å).

Proflavine

Finally, proflavine was modeled with the 3 different-sized carboxylated pillar[*n*]arenes. The cavity of WP[5] is too narrow to allow full binding of proflavine, and instead the dye sits at one portal where binding can be stabilized by a hydrogen bond between the central tertiary amine of the dye and WP[5] (Supplementary Fig. S6).

Proflavine is completely encapsulated within the cavity of WP[6] (Fig. 7). Four hydrogen bonds are observed in the molecular model: 2 at each portal that range in length from 1.87 to 2.50 Å. For WP[7], the larger cavity means the nanocapsule can simultaneously bind 2 proflavine molecules, a feature that is common with the 8 subunit homolog of cucurbit[*n*]uril.[24] While the molecular model of 2:1 proflavine and WP[7] shows only 3 hydrogen bonds, 2 H-bonds at one portal and a single H-bond at the other portal (2.15-2.31 Å), the host-guest complex is also stabilized by a range of other interactions. The 2 proflavine molecules are π-π stacked on each other at a distance of 3.60 Å and there also appears to be π-π stacking interactions between the aromatic rings of WP[7] and the proflavine rings. Two CH-π interactions are also observed between the rings of WP[7] and the aromatic protons of proflavine (3.47 and 3.89 Å). Finally, the 2 proflavine molecules are also shifted slightly

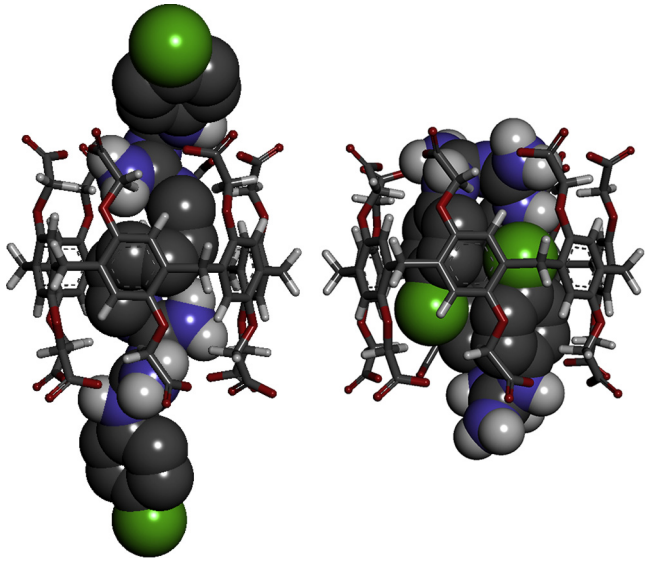

Figure 6. Molecular models of the antiseptic pharmaceutical excipient, chlorhexidine, with (left) WP[6] and (right) WP[7]. The models show how the smaller cavity of WP[6] results in the phenyl groups of chlorhexidine extending through the portals of the nanocapsule, but that the larger cavity of WP[7] allows the chlorhexidine to fold upon itself so that it is totally encapsulated with the nanocapsule.

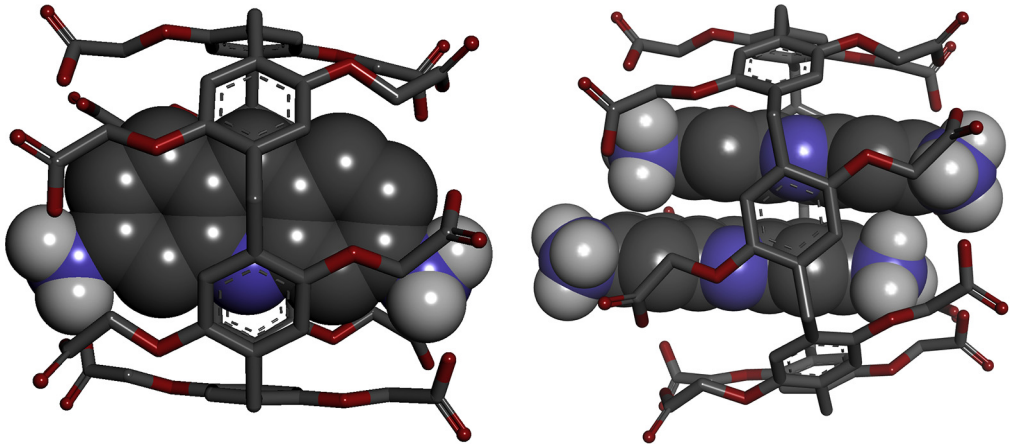

Figure 7. Molecular models of proflavine with (left) WP[6] and (right) WP[7] showing the total encapsulation of the dye within WP[6] and the simultaneous encapsulation of 2 proflavine molecules within WP[7]. For the proflavine-WP[7] 2:1 host-guest complex, the structure is held together through a mixture of hydrogen bonds, π-π stacking between the 2 proflavine molecules and π-π stacking from the WP[7] rings to the proflavine molecules, and CH-π interactions.

to each other along the long axis of the host-guest complex, presumably to minimize electrostatic repulsion between the cationic charges on both molecules.

Binding Strength

The binding strength of the host-guest complexes has been calculated from the molecular models (Table 1). For the 3 carboxylated pillar[*n*]arenes, the binding affinity is seen to increase with nanocapsule size for all 3 guests. The low values for the complexes with WP[5] are consistent with the molecular models where the guests are only weakly associated with the surface or portals of the pillar[*n*]arenes. The increase in binding affinity for all 3 guests moving from WP[6] and WP[7] is also consistent with the molecular models. The increased cavity size of WP[7] compared with WP[6] means the hydrophobic effects can be maximized. The highest binding affinity is for the simultaneous binding of 2 proflavine molecules in the cavity of WP[7] which is again consistent with the molecular model that showed a significant number of interactions between the dye molecules and the nanocapsule that are predicted to stabilize binding.

Importance of Electrostatic Interactions Versus Hydrogen Bonding in Host-Guest Complex Formation

Importantly, carboxylated pillar[*n*]arenes do not form host-guest complexes with all organic compounds that would be predicted to bind into the cavity of the nanocapsules. Albendazole is an antiparasitic drug based on a benzimidazole ring system (Fig. 1). Previously, albendazole has been shown to form host-guest complexes with both cucurbiturils[25,26] and cyclodextrins,[27] and it was predicted that similar binding should occur with the carboxylated pillar[*n*]arenes. However, a 1:1 mixture of albendazole and WP[6] shows no change in the chemical shifts of the albendazole peaks in the ^{1}H NMR, which indicates it does not bind within the nanocapsule (Supplementary Fig. S7).

A similar result is observed for an amine-protected form of the amino acid phenylalanine (Fig. 1). Acetylation of the amino acid's primary amine to an amide means it cannot become protonated, and hence cationic, thus limiting its interactions with WP[6] to just hydrophobic effects and hydrogen bonding. The amino acid forms host-guest complexes with both cucurbit[7]uril,[28] cucurbit[8]uril,[29,30] and α-cyclodextrin,[31] but when mixed with WP[6] there is no change in the chemical shift of the phenylalanine aromatic resonances in their ^{1}H NMR (Supplementary Fig. S8).

Both albenzadole and *N*-acetyl-L-phenylalanine have hydrophobic sections suitable for binding within the cavity of carboxylated pillar[*n*]arenes and amine groups suitable for hydrogen bonding to the carboxylated pillar[*n*]arene portals, but neither compound has a cationic charge to facilitate electrostatic interactions. From these results, it appears that electrostatic binding is more important than hydrogen bonding in forming host-guest complexes with carboxylated pillar[*n*]arenes. To further test this hypothesis, we examined the host-guest potential of acridine orange with WP[6].

Acridine orange is a derivative of proflavine, where the primary amines on either end of the dye have been replaced with tertiary amines (Fig. 1). The pKa of acridine orange is 10.5,[32] which means the dye will be protonated and cationic at physiological pH, and so it can bind to WP[6] via electrostatic interactions. However, its lack of amine hydrogen atoms means binding can not due to the formation of intermolecular hydrogen bonds.

When a 1:1 mixture of acridine orange and WP[6] was analyzed by ^{1}H NMR, the spectra show significant changes to the dye's proton resonances, which broaden and shift significantly upfield by as much as 0.48 ppm (Supplementary Fig. S9). The WP[6] resonances have also significantly broadened and slightly changed chemical shift (0.04-0.09 ppm). The results clearly indicate the formation of a host-guest complex, despite the lack of hydrogen bonding potential of the dye.

When the pH of the acridine orange-WP[6] solution was adjusted to ~14, so that the dye becomes neutral, the solution changed color from orange to yellow and a precipitate formed. The resultant solution contained only free WP[6], which demonstrated

Table 1
Docking Results of Carboxylated Pillar[*n*]arenes (n = 5, 6, and 7) and the Guests: Memantine, Chlorhexidine, and Proflavine

Guest	Carboxylated Pillar[*n*]arene	Binding Affinity (kcal/mol)
Chlorhexidine	WP[5]	−6.6
	WP[6]	−7.3
	WP[7]	−8.9
Memantine	WP[5]	−2.9
	WP[6]	−4.8
	WP[7]	−8.4
Proflavine	WP[5]	−5.7
	WP[6]	−8.2
	WP[7]	−8.0
2 × Proflavine	WP[7]	−10.1

that the dye was ejected from the nanocapsule when it was no longer able to bind electrostatically.

Overall, the results for albendazole, *N*-acetyl-phenylalanine, and acridine orange demonstrate that electrostatic interactions are essential in the formation of host-guest complexes with carboxylated pillar[*n*]arenes, and this must be taken into account when designing drug delivery systems or diagnostic assays.

Fluorescence Quenching

The binding of nanocapsules to dyes can have significant effects on the fluorescence intensity or emission wavelength of the dyes.[33,34] It was therefore of interest to examine the effect of carboxylated pillar[*n*]arenes on the fluorescence of dye: proflavine.

Free proflavine is fluorescent with an excitation wavelength of 451 nm and an emission maximum at 508 nm. Earlier it was shown to form host-guest complexes with both WP[6] and WP[7]. When mixed with WP[6] in ratios of 0-2 proflavine-to-WP[6], there is significant quenching of the dye's fluorescence (Fig. 8), but there was no significant change in proflavine's wavelength of maximum emission. This result is consistent with the binding of paraquat with WP[6], where encapsulation of the compound within the nanocapsule also completely quenched the fluorescence.[35]

Next, we examined the mechanism of quenching. Fluorescence quenching may result due to a wide range of mechanisms, and can be complex if more than one mechanism is involved in the quenching.

Figure 9 shows the Stern-Volmer plot derived via the proflavine fluorescence emission with increasing WP[6] concentration. When a Stern-Volmer plot gives a straight line, then fluorescence quenching is just due to a collisional (dynamic) mechanism. When quenching is due to both collisional and static mechanisms, a Stern-Volmer plot will have an upward curvature. As the Stern-Volmer plot for WP[6] and proflavine curves, then this indicates that more than one quenching mechanism is involved.

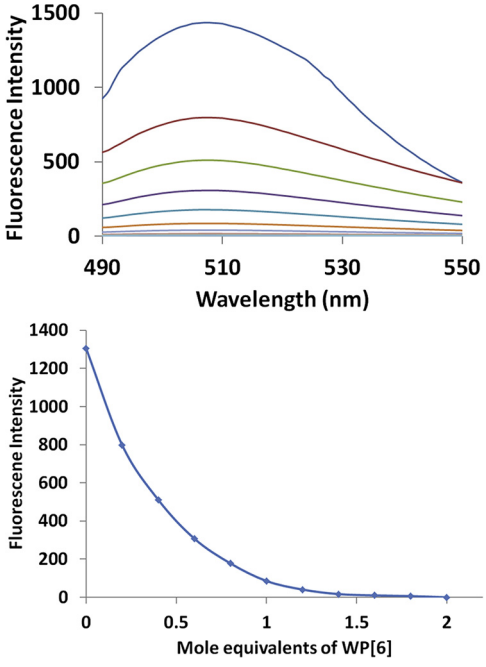

Figure 8. (Top) The fluorescence emission of proflavine (30 μM) in the absence and presence of WP[6] (0-60 μM) showing the progressive quenching that occurs with increasing nanocapsule concentration. (Bottom) a plot of proflavine fluorescence (at 508 nm) as a function of WP[6] concentration.

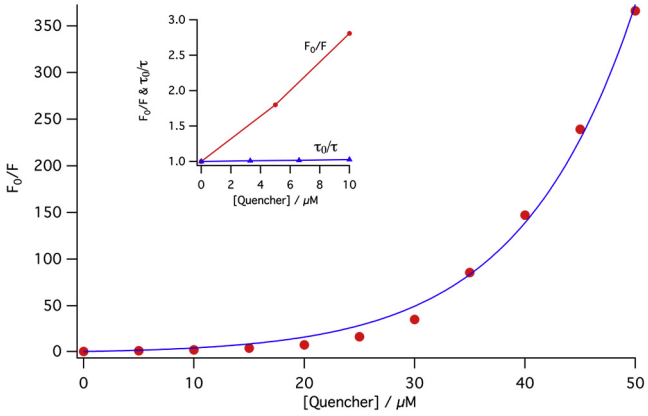

Figure 9. A Stern-Volmer plot of proflavine quenching by WP[6] measured by fluorescence emission (F_0/F) or emission lifetime (τ_0/τ). The solid line is a least squares curve fit to the data with $F_0/F = (1 + K_D Q)\exp(VQ)$. *Inset*: Comparison of proflavine quenching by fluorescence emission and lifetime at representative WP[6] concentrations. Lines are not curve fits.

We also examined the fluorescence lifetime. If collisional quenching is the only mechanism then this is observed through a change in the fluorescence lifetime.[36] Importantly, the fluorescence lifetime of proflavine remains constant (5 ns) with increasing WP[6] concentration, which also indicates that static quenching is a mechanism in this system.[37]

This static quenching is expected when proflavine is encapsulated inside the WP[6] nanocage which results in a nonfluorescent complex. Static quenching occurs only if the molecules are together in the ground state; that is, they are very close to each other or touch each other prior to excitation. We also considered other quenching mechanisms, such as self-quenching by Forster energy transfer; however, due to a small overlap between absorbance and emission spectra this mechanism could be discounted.[38]

Proflavine molecules present in solution and outside the nanocage will still have normal fluorescence when not encapsulated by WP[6]. Nevertheless, increasing the concentration of WP[6] results in reduced dye emission as the number of proflavine molecules that can fluoresce is decreased (Fig. 8).

The Stern-Volmer plot of proflavine quenching by WP[6] was analyzed using the equation $F_0/F = (1 + K_D Q)exp(VQ)$, where K_D is the dynamic component of the bimolecular quenching constant, V is the volume of the quenching sphere—a static component of the quenching, and Q is the concentration of WP[6]. The data analysis gave a K_D of 0.12 ± 0.03 M and a V of 0.08 ± 0.005 M.

Overall, the fluorescence results indicate that the binding of dyes by carboxylated pillar[*n*]arenes may have application as molecular switches with "off" and "on" states when in and out of the nanocapsule's cavities, respectively. Such a system can be applied to the field of biodiagnostics,[39] such as in the sequence-selective recognition of peptides,[40] monitoring drug release,[41] monitoring enzymatic activity,[42] and the detection of nicotine.[43] Based on these systems it is now possible that similar diagnostic tests could be developed with carboxylated pillar[*n*]arenes.

In Vitro *Safety*

In order to have application in medicines for human use, it is important that carboxylated pillar[*n*]arenes are relatively nontoxic.[44,45] So far, most nanocapsule families have been shown to be safe *in vitro*, *in vivo*, and *ex vivo*,[7,44-46] with only β-cyclodextrin

showing any serious toxicity when it is administered via intravenous injection.[7]

Using *in vitro* assays the effect of carboxylated pillar[*n*]arenes on cell confluence was examined over a period of 3 days in the human embryonic kidney cell line HEK293 and the human ovarian carcinoma cell line OVCAR3. As a control, the effect of β-cyclodextrin on cell confluence was also examined.

β-cyclodextrin did not significantly alter the proliferation of either HEK293 or OVCAR-3 cells at concentrations up to 500 μM over 78 h (Figs. 10a and 10c). Carboxylated pillar[6]arene at concentrations ≥25 μM in HEK293 cells and ≥250 μM in OVCAR-3 cells significantly inhibited cell proliferation ($p < 0.01$; Figs. 10b and 10d). Proliferation of the OVCAR-3 cells was significantly inhibited by WP[7] at 78 h and at concentrations ≥100 μM ($p < 0.05$; Fig. 10e). Carboxylated pillar[7]arene was not tested with HEK293 cells.

Overall, the results indicate that both WP[6] and WP[7] are relatively nontoxic to the cells, although they inhibit proliferation at high doses and at extended time periods, whereas β-cyclodextrin did not. Significant effects are only observed at concentrations higher than that would exceed therapeutic doses, and only when the cells were continuously exposed to the nanocapsules over extended time periods. While the biological effects need to be examined in more detail with further *in vitro* and *in vivo* models, carboxylated pillar[*n*]arenes may have application in drug delivery when delivered in small/medium doses over short time periods.

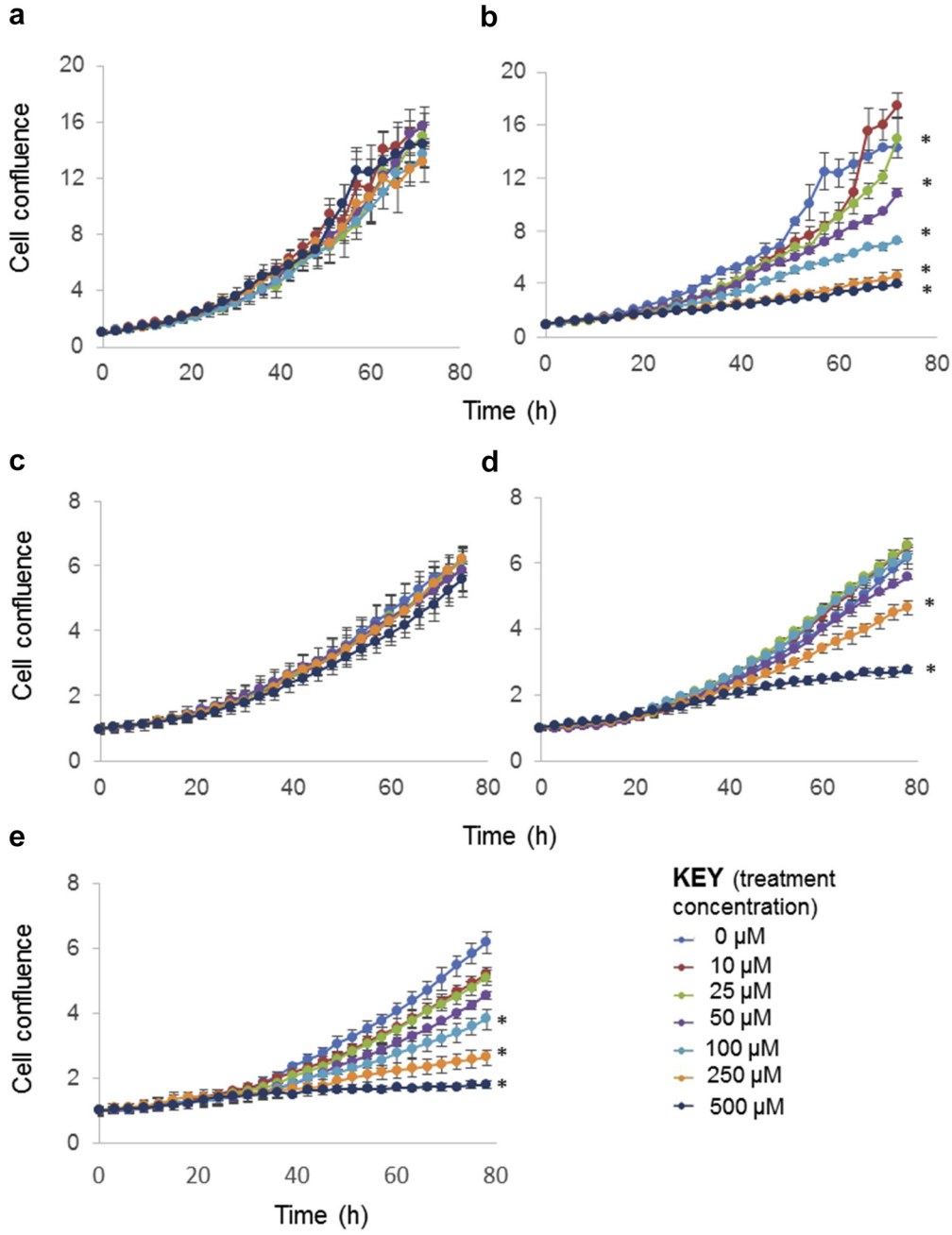

Figure 10. Confluence of HEK293 and OVCAR-3 cells treated with β-cyclodextrin, WP[6], or WP[7] at concentrations between 0 and 500 μM over 78 h showing: (a) HEK293 ± β-cyclodextrin; (b) HEK293 cells ± WP[6] (*$p < 0.01$); (c) OVCAR-3 ± β-cyclodextrin; (d) OVCAR-3 ± WP[6] (*$p < 0.01$); and (e) OVCAR-3 ± WP[7] (*$p < 0.05$).

Conclusions

In this study, the potential of water-soluble carboxylated pillar[*n*]arenes ($n = 6$ or 7) was examined for their ability to form host-guest complexes with a range of biorelevant compounds. Full or partial encapsulation of the guests within the cavity of the carboxylated pillar[*n*]arenes is facilitated through hydrophobic interactions within the cavity, hydrogen bonding between guest amine groups to pillar[*n*]arene carboxylate oxygen atoms, and electrostatic interactions. The results with a range of organic compounds indicate that encapsulation by the carboxylated pillar[*n*]arenes occurs mainly due to hydrophobic effects, and that electrostatic interactions between the host and guest are more important than hydrogen bonding interactions. Binding of proflavine into WP[6] efficiently quenches the fluorescence of the dye giving rise to on and off states.

Despite the *in vitro* results indicating that the carboxylated pillar[*n*]arenes may have some toxicity at very high concentrations and over long exposure periods, they are likely to still have potential biomedical applications because they combine features that solve problems associated with other macrocycle families. These include their easy functionalization (cucurbiturils are very difficult to functionalize), their strong binding to guests (cyclodextrins generally bind guests very weakly), and they have a cavity suitable for the storage and release of drugs (calixarenes have bowel-shaped cavities that do not stabilize and protect drugs to the same extent).

Overall, the results lay the foundation for the novel application of carboxylated pillar[*n*]arenes in drug delivery and biodiagnostics. Potential applications could include the thermal and chemical stabilization of drugs, improvement in drug solubility, as antidotes to poisons and drugs, taste masking, enhancing drug activity, in controlled, slow, or targeted drug delivery systems, and shifting the pKa of drug functional groups.

To develop carboxylated pillar[*n*]arenes for drug delivery and biodiagnostics, further research will need to be undertaken to fully understand the forces and factors involved in drug encapsulation, their safety using further *in vitro* and *in vivo* models, as well as specific studies for each application to be developed.

Acknowledgments

R.R.K. and A.N. acknowledge support of postgraduate awards by the Commonwealth Government of Australia and the University of Sydney.

References

1. Ma X, Zhao Y. Biomedical applications of supramolecular systems based on host-guest interactions. *Chem Rev*. 2015;115:7794-7839.
2. Wheate NJ, Limantoro C. Cucurbit[*n*]urils as excipients in pharmaceutical dosage forms. *Supramol Chem*. 2016 [Epub ahead of print].
3. Da Silva JP, Choudhury R, Porel M, et al. Synthetic versus natural receptors: supramolecular control of chemical sensing in fish. *ACS Chem Biol*. 2014;9(7):1432-1436.
4. Simões SMN, Rey-Rico A, Concheiro A, Alvarez-Lorenzo C. Supramolecular cyclodextrin-based drug nanocarriers. *Chem Commun*. 2015;51:6275-6289.
5. Macartney DH. Encapsulation of drug molecules by cucurbiturils: effects on their chemical properties in aqueous solution. *Isr J Chem*. 2011;51:600-615.
6. Zhou Y, Li H, Yang YW. Controlled drug delivery systems based on calixarenes. *Chin Chem Lett*. 2015;26:825-828.
7. Rowe RC, Sheskey PJ, Cook WG, Fenton ME, eds. *Handbook of Pharmaceutical Excipients*. 7th ed. London: Pharmaceutical Press; 2012:375.
8. Ogoshi T, Kanai S, Fuginami S, Yamagishi T, Nakamoto Y. para-Bridged symmetrical pillar[5]arenes: their Lewis acid catalyzed synthesis and host-guest property. *J Am Chem Soc*. 2008;130:5022-5023.
9. Ogoshi T, Aoki T, Kitajima K, Fujinami S, Yamagishi T, Nakamoto Y. Facile, rapid, and high yield synthesis of pillar[5]arene from commercially available reagents and its X-ray crystal structure. *J Org Chem*. 2011;76:328-331.
10. Chen R, Jiang H, Gu H, et al. A pH-responsive fluorescent [5]pseudorotaxane formed by self-assembly of cationic water-soluble pillar[5]arenes and a tetraphenylethene derivative. *Chem Commun*. 2015;51:12220-12223.
11. Gao L, Zheng B, Chen W, Schalley CA. Enzyme-responsive pillar[5]arene-based polymer-substituted amphiphiles: synthesis, self-assembly in water, and application in controlled drug release. *Chem Commun*. 2015;51:14901-14904.
12. Chang Y, Yang K, Wei P, et al. Cationic vesicles based on amphiphilic pillar[5]arene capped with ferrocenium: a redox-responsive system for drug/siRNA co-delivery. *Angew Chem Int Ed*. 2014;53:13126-13130.
13. Yu G, Yu W, Mao Z, Gao C, Huang F. A pillararene-based ternary drug-delivery system with photocontrolled anticancer drug release. *Small*. 2015;11(8):919-925.
14. Ogoshi T, Hashizume M, Yamagishi T-a, Nakamoto Y. Synthesis, conformational and host-guest properties of water-soluble pillar[5]arene. *Chem Commun*. 2010;46:3708-3710.
15. Lee KKH, Sahin YZ, Neeleman R, Trout BL, Kayser V. Quantitative determination of the surfactant-induced split ratio of influenza virus by fluorescence spectroscopy. *Hum Vaccin Immunother*. 2016;12:1757-1765.
16. Bevington PR. *Data Reduction and Error Analysis for the Physical Sciences*. New York, NY: McGraw-Hill; 1969.
17. Trott O, Olson AJ. AutoDock Vina: improving the speed and accuracy of docking with a new scoring function, efficient optimization, and multithreading. *J Comput Chem*. 2010;31(2):455-461.
18. Danylyuk O, Sashuk V. Solid-state assembly of carboxylic acid substituted pillar 5 arene and its host-guest complex with tetracaine. *CrystEngComm*. 2015;17(4):719-722.
19. Krieger E, Vriend G. New ways to boost molecular dynamics simulations. *J Comput Chem*. 2015;36(13):996-1007.
20. Morris GM, Huey R, Lindstrom W, et al. AutoDock4 and AutoDockTools4: automated docking with selective receptor flexibility. *J Comput Chem*. 2009;16:2785-2791.
21. Sanner MF. Python: a programming language for software integration and development. *J Mol Graph Model*. 1999;17(1):57-61.
22. Fan J, Chen Y, Cao D, Yang YW, Jia X, Li C. Host-guest properties of pillar[7]arene towards substituted adamantane ammonium cations. *RSC Adv*. 2014;4:4330-4333.
23. McInnes FJ, Anthony NG, Kennedy AR, Wheate NJ. Solid state stabilisation of the orally delivered drugs atenolol, glibenclamide, memantine and paracetamol through their complexation with cucurbit[7]uril. *Org Biomol Chem*. 2010;8:765-773.
24. Bhasikuttan AC, Pal H, Mohanty J. Cucurbit[n]uril based supramolecular assemblies: tunable physio-chemical properties and their prospects. *Chem Commun*. 2011;47:9959-9971.
25. Zhao Y, Buck DP, Morris DL, Pourgholami MH, Day AI, Collins JG. Solubilisation and cytotoxicity of albendazole encapsulated in cucurbit[*n*]uril. *Org Biomol Chem*. 2008;6:4509-4515.
26. Saleh Ni, Khaleel A, Al-Dmour H, Yakushenko E. Host-guest complexes of cucurbit[7]uril with albendazole in solid state. *J Therm Anal Calorim*. 2013;111(1):385-392.
27. Pourgholami MH, Wangoo KT, Morris DL. Albendazole-cyclodextrin complex: enhanced cytotoxicity in ovarian cancer cells. *Anticancer Res*. 2008;28(5A):2775-2779.
28. Lee HH, Choi TS, Lee SJC, et al. Supramolecular inhibition of amyloid fibrillation by cucurbit[7]uril. *Angew Chem Int Ed*. 2014;53:7461-7465.
29. Smith L, Leach DG, Blaylock BE, Ali OA, Urbach AR. Sequence-specific, nanomolar peptide binding via cucurbit[8]uril-induced folding and inclusion of neighboring side chains. *J Am Chem Soc*. 2015;137:3663-3669.
30. Rajgariash P, Urbach AR. Scope of amino acid recognition by cucurbit[8]uril. *J Incl Phenom Macrocycl Chem*. 2008;62:251-254.
31. Paduano L, Sartorio R, Vitagliano V, Castronuovo G. Calorimetric and diffusional behavior of the system α-cyclodextrin-L-phenylalanine in aqueous solution. *Thermochim Acta*. 1990;162(1):155-161.
32. Manente S, De Pieri S, Iero A, Rigo C, Bragadin M. A comparison between the responses of neutral red and acridine orange: acridine orange should be preferential and alternative to neutral red as a dye for the monitoring of contaminants by means of biological sensors. *Anal Biochem*. 2008;383:316-319.
33. Saleh Ni, Al-Soud YA, Al-Kaabi L, Ghosh I, Nau WM. A coumarin-based fluorescent PET sensor utilizing supramolecular pKa shifts. *Chemistry*. 2011;52:5249-5254.
34. Wagner BD, Boland PG, Lagona J, Isaacs L. A cucurbit[6]uril analogue: host properties monitored by fluorescence spectroscopy. *J Phys Chem B*. 2005;109:7686-7691.
35. Yu G, Zhou X, Zhang Z, et al. Pillar[6]arene/paraquat molecular recognition in water: high binding strength, pH-responsiveness, and application in controllable self-assembly, controlled release, and treatment of paraquat poisoning. *J Am Chem Soc*. 2012;134:19489-19497.
36. Lakowicz JR. *Principles of Fluorescence Spectroscopy*. 2nd Edn. New York, NY: Kluwer Academic/Plenum; 1999.
37. Kubota Y, Stelner RF. Fluorescence decay and quantum yield characteristics of acridine orange and proflavine bound to DNA. *Biophys Chem*. 1977;6:279-289.
38. Haugen GR, Melhuish WH. Association and self-quenching of proflavine in water. *Trans Faraday Soc*. 1964;60:386-394.
39. Vazquez J, Remon P, Dsouza RN, et al. A simple assay for quality binders to cucurbiturils. *Chemistry*. 2014;20(32):9897-9901.

40. Biedermann F, Rauwald U, Cziferszky M, et al. Benzobis(imidazolium)-cucurbit [8]uril complexes for binding and sensing aromatic compounds in aqueous solution. *Chemistry*. 2010;16(46):13716-13722.
41. Choudhury SD, Mohanty J, Pal H, Bhasikuttan AC. Cooperative metal ion binding to a cucurbit[7]uril-thioflavin T complex: demonstration of a stimulus-responsive fluorescent supramolecular capsule. *J Am Chem Soc*. 2010;132: 1395-1401.
42. Praetorius A, Bailey DM, Schwarzlose T, Nau WM. Design of a fluorescent dye for indicator displacement from cucurbiturils: a macrocycle-responsive fluorescent switch operating through a pKa shift. *Org Lett*. 2008;18:4089-4092.
43. Zhou Y, Yu H, Zhang L, et al. A new spectrofluorometric method for the determination of nicotine base on the inclusion interaction of methylene blue and cucurbit[7]uril. *Microchim Acta*. 2009;164:63-68.
44. Hettiarachchi G, Hguyen D, Wu J, et al. Toxicology and drug delivery by cucurbit[n]uril type molecular containers. *PLoS One*. 2010;5(5):e105014.
45. Oun R, Floriano RS, Isaacs L, Rowan EG, Wheate NJ. The ex vivo neurotoxic, myotoxic and cardiotoxic activity of cucurbituril-based macrocyclic drug delivery vehicles. *Toxicol Res*. 2014;3:447-455.
46. Uzunova VD, Cullinane C, Brix K, Nau WM, Day AI. Toxicity of cucurbit[7]uril and cucurbit[8]uril: an exploratory *in vitro* and *in vivo* study. *Org Biomol Chem*. 2010;8:2037-2042.